

Development and characterization of an eco- friendly cosmeceutical formulation with optimal performance.

Marshall Ringisayi Machingauta

Degree Project in Pharmaceutical Technology, 2022
Department of Physical Chemistry
Lund University
Sweden



Development and characterization of an eco-friendly cosmeceutical formulation with optimal performance.

Marshall Ringisayi Machingauta



LUND
UNIVERSITY

Master Thesis in Pharmaceutical Formulation (30 ECTS credits)
2022

Advisor:
Tommy Nylander
Professor

Examiner:
Marie Wahlgren
Professor

Department of Physical Chemistry
Lund University, Box 124
SE-221 00 Lund, Sweden

Title in popular language

The demand for natural skincare products has seen a sharp rise in the last couple of years. Nowadays, most consumers prefer products that are effective, clean and derived from natural sources in a way that promotes sustainability. However, natural does not always equate to safe, good and effective. Raw materials and ingredients need modification and/or formulation with other components for them to be used to produce skincare products that are good and effective. The biggest challenge for formulation scientists is to make products that ensure that the right amounts of active ingredients can penetrate the skin resulting in the desired benefits.

Shea butter and canola oils are some of the commonly used oils to make skincare products. Shea butter can be processed to divide it into different fractions, these can be used in different quantities and compositions to make skincare products with desired therapeutic and protective properties or as vehicles to deliver active ingredients into the skin. In this work, derivatives of these oils were used to develop a skincare formulation that can be used to heal the skin or protect it from pollutants, ageing and swelling. To achieve this goal, the formulation must have the ability to ensure an optimal amount of bioactive oils penetrate into the skin epidermis. These oils have proven therapeutic benefits in the skin and it is very important that the developed formulation ensures that a high amount is delivered into the skin. To do this, it is important that the inner structure of the formulation is similar to the structure of the inner skin environment.

In this work, various surface-active agents were investigated to determine which one is most ideal for a formulation that has a desired structure. Highly pure soybean lecithin was found to have superior abilities to form the desired structures as compared to the other soybean and sunflower counterparts investigated. Systems containing the lecithin and water (binary system) and systems containing lecithin water and shea butter oil were prepared (ternary system) using compositions of 2 - 40% w/w lecithin. For the ternary system, 15% w/w oil was used in all formulations. Results showed that 2% soy HPC1 was good enough to form desired structures in an oil in water emulsion. Given this, a formulation was developed and the structure was evaluated using various scientific methods. The results of these studies showed that the developed skincare product has the desired structure and therefore can be recommended for use as a highly functional skincare product that meets our objectives. These results can be used as a starting point for further and future development of skin care products that are highly effective. The stability, cosmetic and aesthetic aspects of the product also require optimization therefore further work is necessary to ensure that all the aspects of an ideal product are fulfilled.

Abstract

Cosmetic innovations are about finding high performing creative solutions that deliver into the consumer trends. The consumer trend within the cosmetic industry is currently driving a growing demand for more clean, natural skin care products with sustainable credentials. Enhanced delivery to and interaction with the skin can be achieved through knowledge-based design and characterization of delivery vehicles used for the formulation. The aim of this work was to design and characterize delivery vehicles with enhanced bioavailability and efficacy of bioactive lipids by optimizing the ingredients types and interactions. Firstly, binary emulsifier / water systems, were microscopically characterized and the high purity soy hydrogenated phosphatidylcholine (soy HPC1) produced liquid lamellar phases at compositions of 2 - 40% w/w. Secondly, the ternary phase microstructure of soy HPC1 / water / shea triglyceride system was evaluated using optical microscopy and small-angle X-ray scattering (SAXS). The existence of two-phase regions of liquid lamellar crystalline phase (L_{α}) and cubic phases, single phase regions of (L_{α}) and mixtures of (L_{α}) and gel phases (L_{β}) was observed at investigated concentrations of 2% - 40% w/w of emulsifier with the concentration of shea triglycerides (TG) maintained at 15% w/w. At a low concentration of 2%, soy HPC1 formed L_{α} structures and was chosen as emulsifier of choice for the formulation. The lead formulation was designed with addition of other key ingredients and evaluated. Microscopy and SAXS results of the lead formulation showed L_{α} structures and light scattering showed an average droplet size of 68 μm with high polydispersity. This was considered ideal for enhanced delivery of both photosteroyl canola glycerides and shea butter triterpene esters. The lead formulation was milky in colour, visually slightly viscous with a silky sensorial feeling on the skin. Further work should be done to optimize the formulation, improve the texture and stability and evaluate the functionality.

Keywords:

Emulsifier; lamellar liquid crystals; o/w emulsions; phosphatidylcholine; small-angle X-ray scattering (SAXS); shea butter.

Acknowledgement

The author would like to express sincere gratitude to Prof. Tommy Nylander and Prof. Marie Wahlgren for respectively supervising and examining this work, many thanks go to the Department of Physical Chemistry and Department of Food Technology and Engineering for hosting this work. The author would also like to express sincere gratitude to Dr. Johanna M Borné for co-supervising this work and providing the opportunity to work on this promising project. I am also grateful to AAK Personal Care for funding the project. Many thanks go to Prof. Bjorn Bergenstahl and Peter Holmqvist for all the wonderful conversations we had on this project. Above all, my sincere gratitude goes to the Swedish Institute (S.I) for granting me a scholarship that enabled me to be part of this great institution.

Table of contents

1	List of abbreviations	8
2	Introduction	9
2.1	General objective	9
2.2	Specific objectives.....	9
2.3	Cosmeceutical emulsions.....	9
2.4	Characterisation of emulsions.....	12
2.5	The human skin.....	16
3	Materials and Methods.....	18
3.1	Chemicals	18
3.1.1	Emulsifiers.....	18
3.1.2	Oil phase.....	18
3.1.3	Water Phase.....	18
3.1.4	Bioactive emollients.....	18
3.2	Equipment.....	18
3.3	Methods	19
3.3.1	Phase determination	19
3.3.2	Formulation	19
3.3.3	Microscopy	19
3.3.4	Small-angle X-ray scattering (SAXS).....	20
3.3.5	Light scattering.....	20
4	Results and discussions.....	21

4.1 Screening experiments.....	21
4.2 Binary and ternary phase determination	21
4.3 Ternary Phase	23
4.4 Comparison of emulsifiers	25
4.5 Addition of shea ethyl esters	26
4.6 Addition of stabilisers.....	28
4.7 Addition of bioactive emollients.....	29
4.8 Lead formulation.....	29
5 Conclusions	33
6 Future aspects	34
7 References	35
8 Appendix	38

1 List of abbreviations

PC	Phosphatidylcholine
PL	Phospholipids
LC	Lecithin
L _α	Lamellar liquid crystalline
L _β	Lamellar gel phase
SAXS	Small Angle X-ray Scattering
WAXS	Wide Angle X-ray Scattering
HPC	Hydrogenated Phosphatidylcholine
BPO	Butyrospernum (shea) Parkii Butter Oil
BPE	Butyrospernum (shea) Parkii Butter Esters
BPT	Butyrospernum (shea) Parkii Butter Triterpene Esters
INCI	International Nomenclature Cosmetic Ingredient
SSL	Sodium Stearoyl Lactylate
HLB	Hydrophilic Lipophilic Balance
SC	Stratum Corneum
SLS	Static Light Scattering
DLS	Dynamic Light Scattering
TG	Triglycerides
CA	Cetearyl Alcohol
SF UL	Sunflower non-hydrogenated Lecithin

2 Introduction

2.1 General objective

- The goal of this work is to develop a highly functional dermal delivery vehicle that ensures high bioavailability and efficacy of bioactive emollients.

2.2 Specific objectives

- Exploration of the liquid lamellar phase or any other phase properties formed in the emulsions through the applicative characterization (SAXS, microscopy, light scattering)
- Investigate the effects of emulsifiers and certain key ingredients used in the emulsions and structures formed.
- Based on the experimental results suggest which formulation has lipid self-assembly structures most suitable as delivery vehicle for bioactive emollients.

2.3 Cosmeceutical emulsions

The cosmetic industry continues to grow as the demand for skin care and beauty products is increasing. Cosmetics are preparations that are intended to be used on the body for cleansing, perfuming, beautifying, odorant, and promoting well-being without affecting the structure or function of the body [1]. On the other hand, a cosmeceutical is a product that is applied for personal care and carries both cosmetic and pharmaceutical applications [1]. The cosmetic industry was valued at €76.7 billion in 2020 and the European cosmetics and personal care market is the largest cosmetics market in the world [23]. There is a growing demand for clean and effective products derived from natural renewable sources in an eco-friendly and sustainable way. The market share for green eco-friendly cosmetics in the industry has been increasing in the last couple of years as compared to the conventional synthetic ones. [2]. Current consumer trends within the cosmetic market have seen a rise in demand for more clean and natural skin products with sustainable credentials [3]. On the other hand, there is a fallacy that natural equates to safe, good and effective. This is not necessarily true and natural raw materials need modification for them to be used to produce cosmetic products that are efficacious [3]. To meet this ever-increasing demand, innovative high performing creative solutions are needed to produce products with superior functionalities and improved aesthetics.

Most skin care products that are available on the market are oil in water emulsions made from a mixture of water, emollients, emulsifiers (usually polar lipids), humectants and other ingredients. Their compositions are usually complex as they consist of several components which play a role in controlling the emulsion structure and properties [4]. It is therefore important to understand ingredients individual properties, as well as the possible interactions with other ingredients as these contribute to the nano and microstructures as well as efficacy of the formulations. [3]. Shea (*butyrospermum parkii*) butter and canola oils are two commonly used natural lipid-based emollients in cosmetics. Shea kernels can be processed into many different lipids and some of them contain minor components (triterpenes) with an inherent bioactivity such as anti-inflammatory properties and strengthening of skin barrier function [5]. Lupeol is a well characterized and investigated triterpene that has been found to have a broad spectrum of bioactivities including protease inhibiting, anti-inflammatory, anti-tumour and some minor antimicrobial properties. [5]. The Canola oils contain natural tocopherols (Vitamin E) that are bioactive with anti-oxidative effects, and phytosterols that have anti-inflammatory effects. [3]. The biggest challenge for formulation scientists is to design formulations ensuring optimal bioavailability and efficacy of those bioactive lipids. Given this, enhanced delivery and interaction with the skin can be achieved through knowledge-based design and characterization of delivery vehicles used in formulations.

An ideal cosmetic cream typically should have good aesthetic standards (texture, consistency, convenience to application, odour, colour, fragrance etc.) [3]. One of the most widely used emulsifiers in the cosmetic industry is lecithin and it accumulates at the interface between oil and water, usually forming liquid crystalline structures [6]. Liquid crystals possess both liquid and crystalline properties at the same time and are more organized than liquids, yet less than crystals which makes them good for emulsion stability. They are thermodynamically stable and anisotropic but behaves as two-dimensional fluids [11]. The polar heads are liquid while the hydrated hydrophobic tails are crystalline. Skin lipids in the epidermis are mainly gel state with a high melting point, the stratum corneum consist of lamellar liquid crystals (L_{α}) and lamellar gel (L_{β}) phase giving them a great skin hydration potential [7]. L_{α} structure and properties make lecithins interesting for use in dermal products. Fluid lamellar and lamellar gel phases (L_{β}) are also commonly found in cosmetic emulsions. Fluid and liquid crystalline lamellar are less organised than gel phases [11].

Lecithins are biodegradable and biocompatible amphiphilic molecules with two hydrocarbon chains and a zwitterionic polar headgroup [8]. Lecithins are phospholipids made up of phosphatidylcholine (PC) and a fatty acid chain that can be either saturated (hydrogenated) or unsaturated (non-hydrogenated) and with different chain lengths. Lecithin also contain phosphatidylethanolamine (PE), sphingomyelin (SM), phosphatidic acid (PA) and lysophosphatidylcholine (LP) [9]. LC can be fractionated to produce pure PC (Fig. 1) and the word lecithin is usually used when the product contains less than 80 % by weight total phospholipids, usually PC [10]. The US Pharmacopeia defines lecithin as a mixture of phospholipids (PL) with mainly PC [29]. Most LCs have hydrophilic-lipophilic balance (HLB) value of between 5 and 8, while pure PCs have HLB values of between 9 and 10. [10]. Natural plant-based PLs are efficient emulsifiers over a wide range of ratios of different lipophilic and hydrophilic phases. [10]. PCs can, in contact with water exist in different phases at different temperatures, the temperature and conditions in which a transition occurs from gel phase to liquid-crystal phase depends on the size of the acyl hydrocarbon chain and the saturation/unsaturation [11]. Hydrogenated phosphatidylcholines (HPC) with shorter and saturated hydrocarbon chains are good emulsifiers while those that have unsaturation (non-hydrogenated) on hydrocarbon chains are weak emulsifiers due to the vulnerability of double bonds. [9]. These emulsifiers are amphiphilic and can form different structures in solutions, for example liquid crystals, of hexagonal, lamellar or cubic nature [7]. Furthermore, L_{α} offer ideal consistency and drug delivery, stabilizing effects on emulsions, texturizing effects and skin/bio-mimetic capabilities [12].

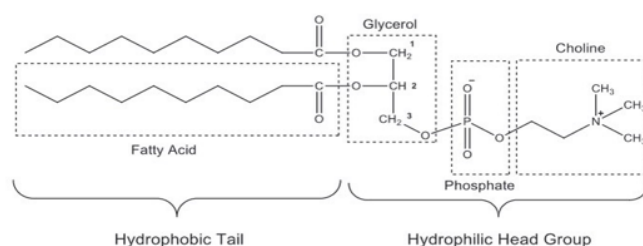


Fig. 1. Molecular structure of a saturated phosphatidylcholine (Adapted from Ref. 13)

Apart from polar lipids like lecithin, non-polar oils (triglycerides) and water are also very important parts used in making a good skin care product, the composition of oil and water in an emulsion determines its stability and cosmetic properties. Among these non-polar oils, derivatives of shea butter like butyrospermum (shea) parkii oil (BPO) and butyrospermum

(shea) parkii butter esters (BPE) are of particular interest due to their biocompatible and biodegradable nature [3]. Mixtures of oil, water and emulsifier at the right temperature leads to phase transitions and formation of emulsions. Hydrocarbons and water are immiscible and phases separate due to different molecular attractions between the phases [11]. Equilibrium of water and hydrocarbon system can be reached when all phases are fluid, however hydrates usually exist as solid crystalline [17]. This makes emulsifiers, temperature and high-speed homogenization important. The Gibbs phase rule is therefore important as it takes into accounts the intensive variables like temperature, pressure, single phase composition, number of components and phases [17]. Different oils show different behaviour in emulsions as a result of their different abilities to interact with the lecithin tails. Polar lipids with longer chain lengths usually form inverse hexagonal phase rather than inverse bi-continuous cubic structure. [6] In addition to this, most cosmetic emulsions also contain other ingredients in order to assure sensorial aesthetic and other cosmetic properties. Given this, the biggest challenged faced in formulation is to understand all the possible interactions between all ingredients in the matrix, and clearly define their effects on the phase diagram [7].

Other commonly used ingredients in cosmetics are polar anionic surfactants. Most of them form micellar phases that are not lamellar and they do not generally affect the pH of the formulation [14]. Sodium stearyl lactylate (SSL) is a biodegradable and biocompatible FDA approved additive with proven excellent stability to coalescence at a relatively low SSL concentration [15]. Mixing two surfactants with two different HLB values can lead to better stability of emulsions, however this may lead to changes in phase behaviour. [7] Given this, the present research focuses on the investigation of possible interactions between the emulsifiers, shea triglycerides, shea ethyl esters, water, cetearyl alcohol and SSL. More so, the addition of alcohol reduces the rigidity of the lipid bilayer structures, makes them flexible and allows the acyl chains to pack better, thereby leading to formation of stable homogeneous emulsions. [6] Understanding of these interactions as well as microstructures can help develop suitable highly functional vehicles for dermal delivery of active ingredients.

2.4 Characterisation of emulsions

Polarized light microscopy is very useful in determining the structural and morphological properties of formulations with high resolution and a small length scale. In optical microscopy visible light is used to provide radiation and one or a series of lenses are used to magnify samples [16]. For samples to be viewed under a microscope, there must be a significant

difference between its refractive index and that of the surroundings [17]. The presence of birefringent objects in polarised light appears as Maltese crosses or shimmering and can be observed using a microscope. Maltese crosses usually indicate an anisotropic L_α phases in the sample [7]. Liquid crystals shimmer under cross polarized light microscopy indicates other birefringent phases like hexagonal, usually with a characteristic fan like pattern, can also be identified using this technique [12]. In addition to this, in colloidal systems, microscopy is also used to identify the shape and particle size and in most of the two-phase systems the particles are not spherical or mono disperse [17]. Most systems are polydisperse and contain a variety of particle sizes hence statistical methods are used to analyse the distribution of the particles sizes [17].

X-ray scattering can be used to evaluate both inter and intra particle structure thereby yielding colloidal and atomic level information respectively [16]. The main advantages of this technique are that it can generate relatively strong signals rapidly and yield relevant data on the Ångström length scale [16, 28]. X-rays are a form of electromagnetic radiation with short wave lengths (λ) of roughly 0.01 to 10nm and a λ of 0.15 nm is typically used to study soft matter like emulsions [18]. These x-rays interact with electrons in the sample therefore this technique probes the distribution of electron density in a sample. Small or wide-angle x-ray scattering can be employed based on the length scale of the colloidal particles of the samples under study in order to obtain information about the inner structure and morphology of the sample [16, 28]. When a beam of an incident electromagnetic radiation hits an emulsion, part of it interacts with the particles and is scattered, while the remainder (transmitted beam) will pass through [16], as shown in Fig. 2. Using SAXS, structural information of particles in smaller length scales can be determined because x-rays have small wavelengths which results in large q ranges [18]. The inverse of q ($\times 2\pi$) gives an estimate of the length scales being evaluated. In this technique, the obtained result is the scattering intensity as a function of q as described by equation below [28];

$$I(q) = N_p V_p^2 \Delta p^2 P(q) S(q) \text{ where;} \quad (2.1)$$

N_p is the number of particles per volume, V_p is the volume of particles, Δp is the difference in scattering length density between solvent and particle, $P(q)$ and $S(q)$ are form factor and structure factor respectively. Generally, scattering information about the particles size and shape can be obtained at low q values, while information about internal structure can be obtained at higher q values.

Based on this, at very low q values where $qR_g < 1$, the Guinier approximation can be used to estimate the R_g (radius of gyration) of the particles based on equation (2.2);

$$I(q) = \Delta\rho^2 N_p V_p^2 \exp(-q^2 R_g^2 / 3) \text{ where;} \quad (2.2)$$

$S(q)=1$, the scattering intensity is based on the zero angle scattering intensity $I(0)$ as shown by equation 2.3.

$$I(Q) = I(0) \exp(Q^2 R_g^2 / 3) \quad (2.3)$$

The q dependence at intermediate q regions of the guinier plot can give information about the shape of the particles, q^{-1} corresponds to cylindrical structure while q^{-2} to lamellar structure [28]. At higher q values the intensity (I) is related to scattering at the surface and a slope of q^{-4} represents smooth surfaces, this is called the Porod region [17]. Using software like SasFit, Igor or SasView for model dependant analysis can help determine the size, shape of particles. X-ray scattering intensity from liquid crystalline phases such as lamellar, cubic and hexagonal leads to diffraction patterns with well-defined peaks as a result of constructive interference [16]. These peaks are called Bragg peaks and they follow the Braggs law as shown by the equation (2.4) below [18];

$$n\lambda = 2d \sin (\theta/2) \quad (2.4)$$

where n is an integer (diffraction order), d is the distance between lattice planes and θ is the scattering angle. The characteristic distance of the interplane can be calculated using equation (2.5) [18];

$$d = 2\pi/q \quad (2.5)$$

Liquid crystalline structures can be determined by the ratios of different Bragg peaks of the particles where lamellar is q ratio 1:2:3, hexagonal is $1:\sqrt{3}:2$. Cubic phases can be bi-continuous or micellar and both can be further subdivided into various types [16].

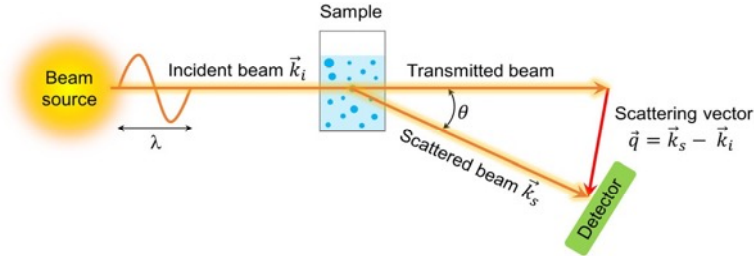


Fig. 2. Schematic presentation of a scattering experiment, \vec{q} is the scattering vector, θ is the scattering angle. (Adapted from Ref. 28)

Laser light scattering is commonly used to study droplet sizes in emulsions, however, it is only suitable for very dilute systems ($\phi < 0.05$ wt %) [24]. In this technique, the radiation source is a laser beam of monochromatic plane polarized light that has a wavelength in the visible range [24]. At any angle the intensity of the light scattered light is dependent on the wavelength of the incident light, optical properties of the scatterers, angle of observation as well as the shape and size of the particles under study [17]. The radius of gyration R_g of the oil droplets can be determined from the angular dependence of the scattering intensity as a spatial and time average [16]. The measurements can be done at scattering angle θ° where $0^\circ < \theta < 180^\circ$ and this depends on the geometry of the specific instrument. Assuming that the conditions for Rayleigh scattering applies, scattering objects smaller than wavelength of the radiation, the beam is scattered when hits and object in a sample, it is scattered and appears attenuated compared to the incident light. [17]. Light intensity is defined as the radiation energy that hits a unit of area in time unit and is proportional to the square of the electric field of the radiation. The total amount of light transmitted is the summation of all the light scattered at the probed angles, which is measured in static lights scattering. [17]. In this work, we also used dynamic light scattering whereby the fluctuation in scattering intensity, due to Brownian motion, is measured at a specific angle. The data are analysed with help of a time correlation function, which gives a characteristic decay time that gives the mobility of the particle. The scattering intensity is normalized against a reference e.g. toluene, and this is expressed as the excess Rayleigh ratio (ΔR_θ) [18]. The molecular weight and size of particles are all related with this ratio and can be expressed as;

$$\Delta R_\theta = KMCP(q)S(q) \quad (2.6)$$

where K is the optical constant related to instrument set up and sample, C is the solute mass concentration, $P(q)$ is the form factor expressing intraparticle interference effects, $S(q)$ is the structure factor representing contribution of interparticle interference of scattering intensity

[28]. For dilute samples of small particles, the scattered intensity is independent of the scattering angle and for non-interacting large particles is dependent on scattering angle [28]. The dependence on the scattering angle is directly proportional to particle size and the size and shape of the particle is reflected on the form factor $P(q)$ [16]. The particle size distribution and polydispersity on a two-phase system can also be determined using data from light scattering [19]. Polydisperse index (PDI) is a dimensionless and scaled value calculated from a 2-parameter fit to correlation data, values higher than 0.7 indicate that the sample has a very broad size distribution [19].

2.5 The human skin

The skin is the biggest part of the human body and plays a crucial role in holding the integrity of the body and internal homeostasis normal [25]. Given this, it acts as physical barrier against hostile environmental pollutants and also prevents excessive water loss from the body [20]. The skin (Fig. 3) is made up of layers and the epidermis is the outer most layer which is subdivided into viable epidermis, dermis and hypodermis (subcutaneous layer) [21]. The epidermis is composed of the stratum corneum which has an intercellular matrix composed of lipid lamellae layers in an aqueous environment. [21]. The multilayer arrangement of lipids in the skin provides a good barrier against strongly polar and strongly nonpolar substances, some of which may penetrate skin. [22]. Damages to the epidermis due to light exposure, pollutants, diseases, inflammation and aging can impair the skin's ability to perform its barrier function [21]. Changes in the lipid components of the stratum corneum and pH can lead to severe skin dehydration and trans epidermal water loss [22, 25]. Changes in hydration impacts the lipid crystalline packing and fluidity, this affects the skin's ability to perform its functions [21] This gives it a rough and scaly appearance and consequently leading to a loss of mechanical properties. Skincare formulations containing lamellar phases can therefore be used to aid in this barrier function. Furthermore, some researchers observed sustained release of both hydrophilic and lipophilic drugs using dermal formulations with lamellar structured inside [7]. Drug release from swollen liquid crystalline structures was also observed to be slow compared to formulations with hexagonal phases [7]. Scientists in the cosmetics industry develop emulsions which can be used to preserve skin integrity as well as prevent and/or treat skin disorders.

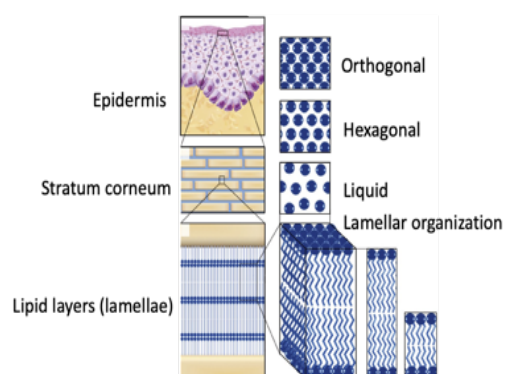


Fig. 3. The intercellular matrix found in the stratum corneum, composed of lamellae lipid layers between the corneocytes. (Adapted from Ref. 20).

Most researches focus on studies of how the properties of skin can be altered by additives like moisturizers, penetration enhancers etc. leading to increased permeability of active ingredients [22]. However, most formulations often have complex compositions making it hard to determine the effects of certain ingredients. It is therefore important to formulate a clean (few ingredients from same source) cosmetic formulation that is highly functional. This enables us to observe and understand how specific ingredients affect the formulation and efficacy of the formulation. The results of this work can therefore be used to fill in the knowledge gap on the emulsions prepared by combinations and types of ingredients used in this work, such information can be valuable for future development of dermal preparations.

3 Materials and Methods

3.1 Chemicals

All chemicals and/or ingredients used in this work were of cosmetic grade and were used without further purification. The list of all ingredients used is found in Appendix A below

3.1.1 Emulsifiers

Soybean and sunflower emulsifiers (phospholipid) were provided by AAK Personal Care. Four different types used in this work were soy hydrogenated phospholipid with medium purity (amount of phosphatidylcholine), soy hydrogenated phospholipid high purity (amount of phosphatidylcholine), soy non-hydrogenated lecithin, sunflower non-hydrogenated lecithin. All phospholipids were powdered and deoiled and were used without further purification. Other surfactants used were cetearyl alcohol (C16-18) surfactant from BASF and sodium stearyl lactylate from AAK Personal Care.

3.1.2 Oil phase

Two oils used in this work were butyrospermum parkii (shea) butter triglycerides and butyrospermum (shea) butter ethyl esters, both were provided by AAK Personal Care.

3.1.3 Water Phase

Deionized passed through a purification system (Milli-Q, Burlington, MA, USA) to obtain water with a resistivity = 18.2 mΩ.cm, organic content < 4ppb.

3.1.4 Bioactive emollients

Two bioactive emollients investigated in this work were photosteryl canola glycerides and butyrospermum parkii butter (shea butter triterpene esters), both provided by AAK Personal Care.

3.2 Equipment

The oil in water emulsions were mixed using an Ultra Turrax T25 high speed homogenizer (IKA, Freiburg, Germany), the temperature was controlled by a self-adjusting Grant Boekel BBD4 heating block and a thermometer, X-ray scattering was conducted using SAXSLAB Ganesha 300 XL (JJ Ray, Denmark). Light scattering was done using Malvern Zetasizer Nano

ZL (DLS) and Malvern Mastersizer 2000. Data was processed using Zetasizer software version 7.12 and mastersizer 200 software version 5.6, respectively. Microscopy was done using Olympus BX50 equipped with a ImagingSource DFK41AF02 camera. IC Capture 2.4 and Image J softwares were used to view and capture the images as well as measuring length scales. Milli Q Gradient A10 was used to purify the water while Mettler AE160 scale was used to weigh the samples.

3.3 Methods

The different methods used in the preparation and analysis of samples are described below.

3.3.1 Phase determination

For phase determination, binary systems were prepared by separately heating HPC or LC (2%, 5%, 10%, 20%, 40% w/w) and water to 80°C and then mixing the phases while homogenising at high speed. Samples for ternary phase determination were made using the same compositions of HPC, and 15% w/w of shea TG was added in all samples. Shea TG and soy HPC1 were weighed and mixed before heating to 80°C then adding to hot water (80°C) while mixing. Phases formed were determined using microscope and subsequently x-ray scattering.

3.3.2 Formulation

The oil and emulsifier were weighed and mixed in a bottle before heating to 80°C, the water was weighed and added to a separate bottle and heated to the same temperature. The two phases were mixed and homogenised using ultra turrax (6500 rpm) for 5 minutes. The emulsions were allowed to cool to 25°C while stirring. Various compositions of samples were prepared as shown in Appendix B.

3.3.3 Microscopy

A few drops of the emulsions were spread thinly onto the glass slide using a micro spatula. A thin cover glass was placed on top of the sample to avoid evaporation prior to analysis. The structure of the samples was examined under microscope using an Olympus BX50 at 25 °C. The magnification used was 20X under polarized light in order to investigate the presence of liquid crystalline phases in all the samples. IC Capture 2.4 and Image J software was used to process and analyse the obtained micrographs.

3.3.4 Small-angle X-ray scattering (SAXS)

The X-ray scattering experiments were done using SAXSLAB GANESHA 300 XL, which was equipped with microfocus sealed X-ray source and a Pilatas solid state 2D photon counting detector. The voltage and anode current were set at 50 kV and 0.6 mA respectively. A wavelength of $\lambda = 1.54 \text{ \AA}$ was used and the scattering vector q was calculated as $q = (4\pi \sin\theta)/\lambda$ where θ is half the scattering angle. The samples were pipetted into a quartz capillaries and measurements were performed at 25°C and 35°C using configurations 21 (q ranges 0.1 – 2.75 \AA^{-1}), 22 (q ranges 0.023 – 0.73 \AA^{-1}) and 23 (0.005 – 0.30 \AA^{-1}), at measurement times of $t = 600$ s, 3600 s and 7200 s respectively. The results were processed using SasView modelling software and the interlayer spacing (d) was calculated using $d = 2\pi/q^1$ where q^1 is the value of the scattering vector at the first peak maximum in the scattering curve.

3.3.5 Light scattering

Light scattering was performed using two instruments, Zetasizer Nano ZS (DLS) and Metasizer 2000 (SLS). For the metasizer 2000 a rapeseed refractive index of 1.47 and 1.33 for water was used at a laser obscuration of about 7%. A few drops of samples were added into the water in the equipment and stirred prior to analysis, the lipid concentration was approximately 0.5mg/ml. The total scattering intensity (I_{tot}) was measured and an average of consecutive triplicate measurements was recorded. Data was processed using mastersizer 200 software version 5.6. The Zetasizer utilized back scattering geometry at a scattering angle of $\theta = 173^\circ$ using same refractive indices as the ones used on the masterzizer. The samples were diluted 200-fold prior to analysis in a standard disposable cuvette at a temperature of 25°C. The total scattering intensity (I_{tot}) was measured and an average of consecutive triplicate measurements was recorded. Data was processed using Zetasizer software version 7.12.

4 Results and discussions

4.1 Screening experiments

During the early stages of formulation development various samples were prepared and evaluated visually and with a microscope to determine the optimum type and amount of emulsifier required to form homogeneous emulsions with desired structures. Binary and ternary sample prepared using soy HPC1, soy HPC2 and soy UL formed good o/w emulsions. However, samples made using sunflower non-hydrogenated lecithin (SF UL) formed non-homogeneous systems in all compositions investigated. As a result, this emulsifier was deemed difficult to handle and discontinued. Unsaturated phospholipids usually are sticky, hygroscopic and challenging to handle, whereas saturated natural phospholipids, especially grades with at least 90% phosphatidylcholine have good powder flow properties [13]. The other reason why SF UL was difficult to handle is that it was crude and contained slightly high amounts of phosphatidylethanolamine (PE), phosphatidylinositol (PI), phosphatidylserine (PS) and phosphatic acid (PA). These different lipids have different melting temperatures and this leads to them organising poorly in an emulsion. The purity and grade of lecithin are very important determinants for its function [10], they have an effect on melting temperature, packing and overall potency of the emulsifier. Soy HPC2 produced emulsions that were more homogenous, visually appeared viscous and stable than those prepared using soy HPC1. According to F Otto et al, unsaturated PE molecules have an inverted cone shape, making them wider at the top and narrow at the bottom [10]. This makes them fit better into the curvature of the interface of o/w emulsions [10], this might explain why formulations made using soy HPC2 were more homogenous and stable than those made using soy HPC1. Generally, natural PLs with a higher concentration of PE exhibit a lower HLB range hence can be more suitable for o/w emulsions [10, 26]. However, PLs with the highest HLB-range are considered best for preparation of o/w-emulsions [10]. Based on the thorough screening, soybean lecithins were chosen for further evaluation.

4.2 Binary and ternary phase determination

The results from investigating the phase behaviour of all the three emulsifiers investigated are shown in Table 1 below and Appendix D. Results showed purified HPC formed L_{α} at lower amounts compared to non-hydrogenated lecithin. Soy HPC1 formed L_{α} phases from 2% – 40% w/w compositions while soy HPC2 formed L_{α} phases from 5% – 20% w/w. Fig. 4 below shows

polarized microscopy images of the different phases formed. Fig 4a shows microscopic images indicative of isotropic micellar or bi-continuous cubic phases. Maltese crosses texture indicative of lamellar phase (Fig. 4b and c) were observed for samples with the L_{α} region while a more ordered lamellar (Fig. 4d) was observed for samples with 40% w/w HPC content. From 2% – 40% w/w soy HPC1, a L_{α} dispersed in water was observed, coexistence with cubic phase was later confirmed using SAXS. According to Montalvo, G. et al, the stability of the lamellar phase extends to even lower concentrations of PC and this was observed in samples prepared using soy HPC1 [6]. Formulations made using soy HPC2 and soy UL formed isotropic phases (Fig. 4a) at 2%, w/w and the types of phases formed at higher concentrations are shown in Appendix D. As a result, soy HPC1 emulsifier was selected for further evaluation of phases formed in a ternary system. At low emulsifier compositions (5% w/w) isotropic phases, likely cubic, and mixtures of two phases (C+L) were also observed in soy UL and soy HPC2 samples respectively. At higher compositions (10 – 40% w/w) of emulsifiers L_{α} structures were observed. We note that from the polarized microscopy images it is not possible to identify the structure of the isotropic particles, although they are likely to be cubic. To confirm that the structures were cubic, x-ray scattering experiments were performed and the results are discussed in detail below.

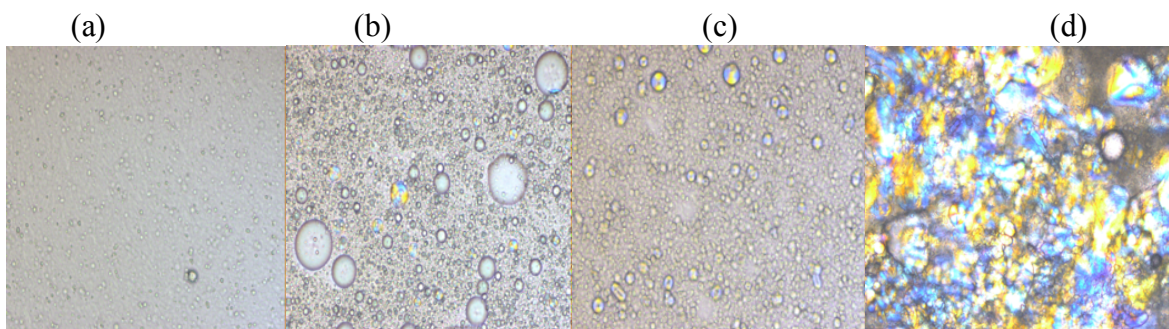


Fig. 4 Microscopic images showing (a) isotropic phases, (b) liquid lamellar + isotropic phases (c) liquid lamellar phases (d) lamellae (L_{α} and gel (L_{β}))

Table 1. Phases formed by different concentrations of binary systems prepared using soy HPC1 and water, the phases are identified using microscopy and SAXS.

	Micellar Cubic (C)	Lamellar (L)	Lamella gel (G)	Mixed C + L	Mixed L + G
Soy HPC1 % in water					
2				✓	
5				✓	
10		✓			
20					✓
40					✓

4.3 Ternary Phase

A pseudo-ternary phase diagram (Fig. 5) of soy HPC1/shear TG/water system at 25°C, was determined by a combination of optical microscopy with crossed polarizers and SAXS. The ternary system shows a predominantly fluid isotropic/cubic phase coexisting with anisotropic L_α at low emulsifier (2% – 5 % w/w) concentration and L_α phases at 10%. At 20% and 40% w/w soy HPC1, a multiphasic region, where other lamellar phases like gel (L_β) phase coexisted with L_α phases were observed. Montalvo G et al posits that the existence of areas of phase coexistence (hexagonal, cubic and lamellar liquid crystalline phases) in ternary systems of oil, lecithin and water is as a result of the low miscibility of the oil in the lecithin bilayer and the segregation of the phospholipid polydisperse hydrophobic chains [6]. Point *a* in the phase diagram represent a two-phase region with a mixture of L_α and bi-continuous cubic phases. From 5% to 15% w/w of emulsifier (points *b, c, d*,) L_α domains dispersed in isotropic bulk are clearly identified by optical microscopy and confirmed by SAXS. A two-phase region of L_α and gel phases (points *e*, and *k*) was observed at 20 and 40% w/w soy HPC. SAXS results to confirm these structures are shown in Fig. 6.

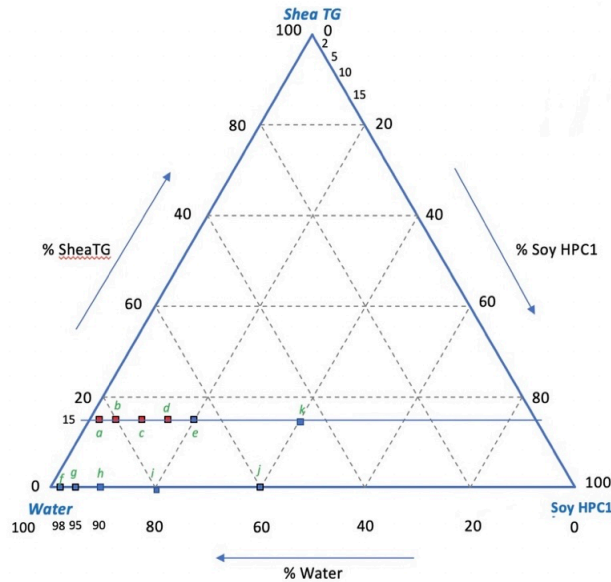


Fig. 5. Phase diagram for the soy HPC1/shear TG/water system at 25°C. Points *c* and *h* in the ternary phases show L_α region and points *g* to *e*, *i*, *j* and *k* show L_α and gel phases. Points *a*, *b*, *g* and *f* show L_α and cubic two-phase region. Solid lines indicate fixed ratio compositions of measured samples. Blue and red squares correspond to the experimental points discussed in the data analysis.

Liquid crystalline phases form one, two, or three-dimensional structures and SAXS curves show Bragg peak intensities for specific values of the scattering vector q [8]. Fig. 6 below shows SAXS data for binary and ternary samples. All of the studied samples show the presence of lamellar phases characterized by Bragg peaks at q positions 1:2:3. The curves for the binary system (Fig. 6a) show a mixture of cubic (Bragg peak ratio of $\sqrt{3}$, $\sqrt{8}$, $\sqrt{11}$) and lamellar phases at low concentrations of emulsifier, the system becomes predominantly lamellae at higher concentrations of emulsifier. At 2% w/w soy HPC1, the SAXS patterns showed less defined broad peaks, the shoulders of the peaks were consistent with Bragg peak ratios for L_α structures (1:2:3). Given the isotropic phases observed in microscopy, it is therefore plausible that some peaks to confirm cubic phases were hidden in the broad peak. Although the peaks in the binary system SAXS data (Fig. 6a) are more defined and sharper with increasing concentration, results of all the investigated samples showed L_α orientation as reflected by q ratios of 1:2:3 in all curves (1,2,3,4,5 in the image). The position of the peaks did not shift at all concentrations investigated thereby showing that the lamellar phases were dominant and/or present in all the samples analysed. The peaks became sharper with increasing concentration and this shows the existence of more solid crystals or lipids at high concentrations, these observations correspond with the results of microscopy and visual inspections where solid crystals were observed.

For the ternary phase samples (Fig 6b), an additional peak (b) was observed at $q = 0.14 \text{ \AA}^{-1}$, this is indicative of an additional phase in the system which can be a gel phase. The results of the ternary system samples showed that the addition of shea TG slightly affected the nanostructure of the system. Although the peaks were slightly broader than those of binary phases, distinct peaks with q ration (1:2:3 for peak a,c,d) representing L_α orientation were observed. An additional peak was observed at point b shown in the images, this peak became sharper at high concentration. This peak could also represent crystals or solid lipids in the formulation given how sharp it is especially a higher PL concentration. The peak broadening (Fig. 6b) observed after addition of shea oil can also be interpreted as showing a form factor of vesicles. This can be indicative of ordered multi lamellar vesicles formed in the system as the emulsifier circles around spherical shea TG droplets. The interlayer spacing (d) was 69 \AA , calculated as $d = 2\pi/q^1$ where q^1 is the value of the scattering vector at the first peak maximum in the scattering curve. This means that the distance between repeating crystal lattices or layers in the system was approximately 69 \AA .

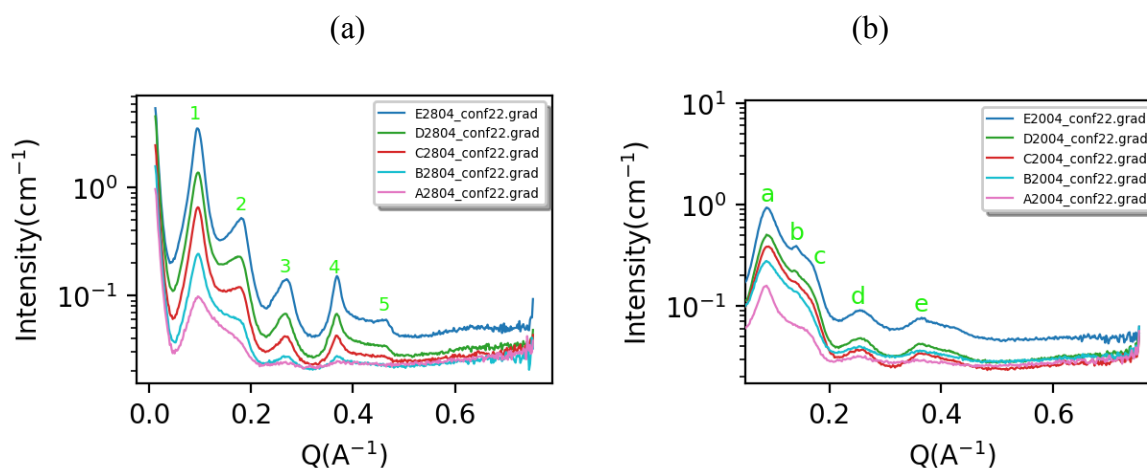


Fig. 6. SAXS curves showing phases formed in binary systems (a) and phases formed in ternary systems (b). A, B, C, D, E2804 represent 2,5,10,20,40% soy HPC respectively in the binary system, while A, B, C, D, E2004 represent 2,5,10,20,40% soy HPC respectively in ternary system with 15% shea TG. Points 1-5 in (a) represent Bragg peaks showing q ratio 1:2:3:4 for L_{α} and points a-e in (b) represent Bragg peaks (L_{α} being a,c,d,e), point b observed at high soy HPC concentrations indicate an additional phase or solid crystals in the system.

4.4 Comparison of emulsifiers

Fig. 7 below shows SAXS diffractogram for samples made using the 3 different emulsifiers (soy HPC1, soy HPC2 and soy UL) at 5% w/w.

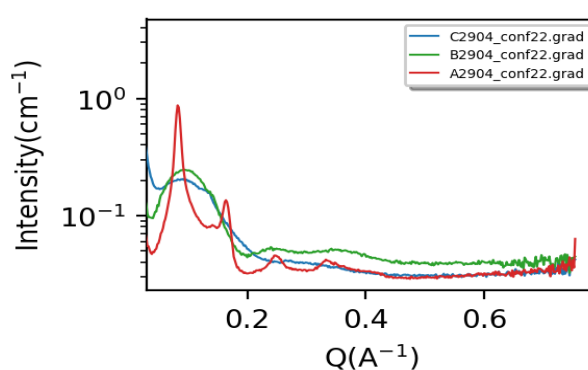


Fig 7. SAXS curves for formulations A2904 (soy HPC1), B2904 (Soy HPC2), C2904 (Soy UL). All 3 formulations had distinct SAXS patterns and microstructure.

SAXS results for formulation made using soy HPC1 (A2904) clearly showed Bragg peaks corresponding to a L_{α} phase. On the other hand, soy HPC2 and soy UL showed broad peaks

which could indicate the form factor of spheres overlapping the structure of a L_{α} phase. Broad peaks can also be an indication of a more fluid and less crystalline structure in the system and this corresponds with results from visual inspection of the formulations. For soy HPC2 (B2904), there is a broad peak that is accompanied by 2 other peaks showing Bragg peaks corresponding to a L_{α} phase, this could mean that the L_{α} orient into vesicles, these observations corresponds with those from microscopy where we observed maltese crosses and shimmering in the sample.

4.5 Addition of shea ethyl esters

The addition of shea ethyl esters in the system is done to improve the texture and sensory feel of the formulation to improve cosmetic and aesthetic properties [3]. As expected, the addition of 5% of the ester appears to increase viscosity of the system based on visual inspection, a silky and cushion feel was also observed when the formulation was applied to the skin. Droplet sizes of formulations with and without the shea ethyl esters were evaluated using light scattering. SLS analysis gave the information about the droplet size and distribution, all the emulsions presented a monomodal polydisperse distribution, however, the lead formulation was less homogeneous with a polydisperse size distribution. Fig. 8 below shows the average droplet sizes for samples analysed using SLS. In formulations with soy HPC1 as the emulsifier (A0704 and C2203), addition of shea ethyl esters led to a reduction in average droplet size as shown in the histograms in Fig. 8 below and microscopic images in Appendix H. In formulations with soy HPC2 (A1404 and F2203) and soy UL (B1404 and B2303), the addition of shea ethyl esters led to slight increases in the average droplet sizes.

In another study by F Otto et al, the investigated emulsions prepared with natural PLs had a non-Gaussian size distribution of the oil droplets and the size distribution [10], this was observed in all the emulsions we investigated. However, emulsions made using soy HPC1 had the highest polydispersity and a tendency for phases to separate. The possible explanation for this behaviour may be the different affinity of PC to the used oil phase. This could be due to the differences in their respective structure, chain length and saturation and hence the resulting interactions at the interface. However, based on visual observations, the addition of the shea ethyl esters appeared to increase the viscosity and reduced phase separation. Table 2 below shows the average droplet sizes for all samples using SLS, DLS and microscopy. DLS measured the sizes of the vesicles formed and the polydispersity index (PDI) as shown in table 2 below. Formulations made using soy HPC1 had average vesicles of approximately 427 and 344nm for formulation made with and without shea ethyl esters respectively. The polydispersity index was

more than 0.9 for both formulations meaning high polydispersity amongst that population. The polydispersity for formulations made using soy HPC2 and soy UL was slightly lower (PDI \approx 0.59) than that of the soy HPC1 (PDI \approx 0.67). Although the PDI is a measure of polydispersity, the results are not a good reflection of the sample since this technique only measures particles less than 1 μ m, most of the particles in our sample are significantly larger than that. The scattering of the light is also affected by the big particles in the sample thereby making the results less reliable.

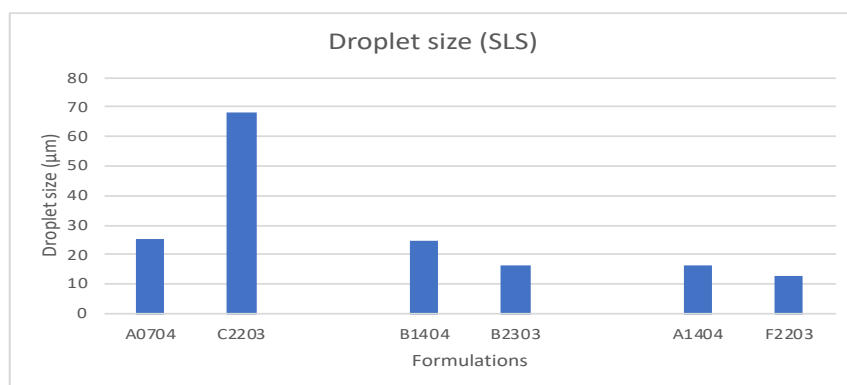


Fig. 8. Comparison of droplets sizes for formulations prepared with and without ethyl esters using all 3 emulsifiers. More information about the emulsions is given in Table X below

Table 2. Average droplets sizes for formulations prepared with and without shea ethyl esters for all 3 emulsifiers. Droplets sizes measured using SLS, DLS and microscopy.

Emulsifier used	Formulation	Shea butter ethyl ester	SLS (μ m)	Microscopy (μ m)	DLS (nm)	PDI (DLS)	Polydispesity
Soy HPC1	A0704	With	25	29	427	0.91	high
	C2203	Without	68	44	344	0.98	very high
Soy UL	B1404	With	24	23	213	0.61	medium
	B2303	Without	16	12	338	0.67	medium
Soy HPC2	A1404	With	16	18	828	0.59	medium
	F2203	Without	12	15	738	0.66	medium

In addition to this, based on SLS, emulsions prepared using soy HPC1 had the biggest average droplets sizes compared to the emulsions prepared using the other 2 emulsifiers. In emulsions prepared by hydration of PCs, the particle size is affected by length and degree of unsaturation of the hydrocarbon chains, the emulsifier with shorter acyl hydrocarbon chains or unsaturated acyl chains are more potent dispersing agents while those with short saturated acyl hydrocarbon

chains are better emulsifiers [9, 24]. Better emulsifiers lead to smaller droplets, high viscosity and stable emulsions. Surprisingly, soy HPC1 produced emulsions with the biggest average droplet sizes, low viscosity and stability compared to the other 2 emulsifiers. The possible reason for this is poor interaction with the oil at the droplet interface.

4.6 Addition of stabilisers

The addition of SSL and cetearyl alcohol (CA) led to formulations that visually appeared more viscous and stable. O/W emulsions prepared using SSL shows excellent stability to coalescence, and this can be observed using relatively low amounts SSL [14]. Visual observations of the formulation prepared with these 2 ingredients showed that the formulation phases did not separate after 90 days. This was contrary to formulations without the added stabilizer. The SSL adsorbs at the oil and water interface thereby stabilising the emulsion. According to Kurikji et al, a higher interfacial tension is observed at slightly higher SSL concentration in an oil in water emulsions [14], however, very high concentration of SSL leads to lower interfacial tension. The SSL used in this work has an HLB value of 17 and this makes it a very potent polar non-ionic surfactant [3]. Given this, good emulsion stability was observed at relatively low concentrations (0.3 and 0.5 w/w%) investigated. Fig. 9a below shows SAXS results for formulations made with and without SSL and CA. The images (Fig. 9a) showed a wide peak (G1403) and additional Bragg peaks showing a form factor of vesicles and L_{α} phase. Peak broadening shows that the system was more fluid and less crystalline, this was also confirmed using visual inspection of the formulation. The ratios for q ratios showed the presence of an L_{α} phase and therefore it can be concluded that these 2 ingredients stabilised the lamellar structures into ordered vesicles.

The results for formulations without SSL show narrow and sharp Bragg peaks indicative of a more defined L_{α} . According to Kurijki et al, SSL has a propensity to form highly ordered, stable bilayer aggregates in an aqueous media, this phenomenon was observed in formulation G1403 investigated in this work. The spherical multi lamellar vesicle structures also showed a relatively bigger d spacing compared to the samples without SSL. Given this, the addition of SSL significantly changes the nanostructure of the emulsions away from a well-defined L_{α} phase. Although SSL improves the stability of the system, the changes in the microstructure might affect the dermal delivery and bioavailability of the bioactive emollients. L_{α} phase structures have been proven more ideal for better dermal delivery [8]. On the other hand, the addition of cetearyl alcohol did not significantly change the nanostructure of the emulsions.

SAXS data show that the emulsion nanostructure remained the same after addition of CA. The cetearyl alcohol is known for its ability to form lamellar phases in emulsions. [7]. Furthermore, based on visual and sensorial observations, the addition of this ingredient slightly improved the viscosity, texture and stability of the emulsion.

4.7 Addition of bioactive emollients

Phase and structural changes due to addition of the of the bioactive emollients were also investigated. Fig. 9b shows SAXS data for formulations with (A0304) and without (B0304) the bioactive emollient. As shown in Fig 9b, addition of shea triterpene esters and photosteroyl canola glycerides did not change the microstructure of the emulsions, the SAXS curves were the same for samples with and without the bioactive emollient. Clean system made from ingredients with the same INCI are likely to produce a more potent and stable emulsion with a more defined lamellar structure. Although the photosteroyl canola glycerides have a different INCI name and chain length than shea TG, adding it to the system did not change the nanostructure of the emulsions.

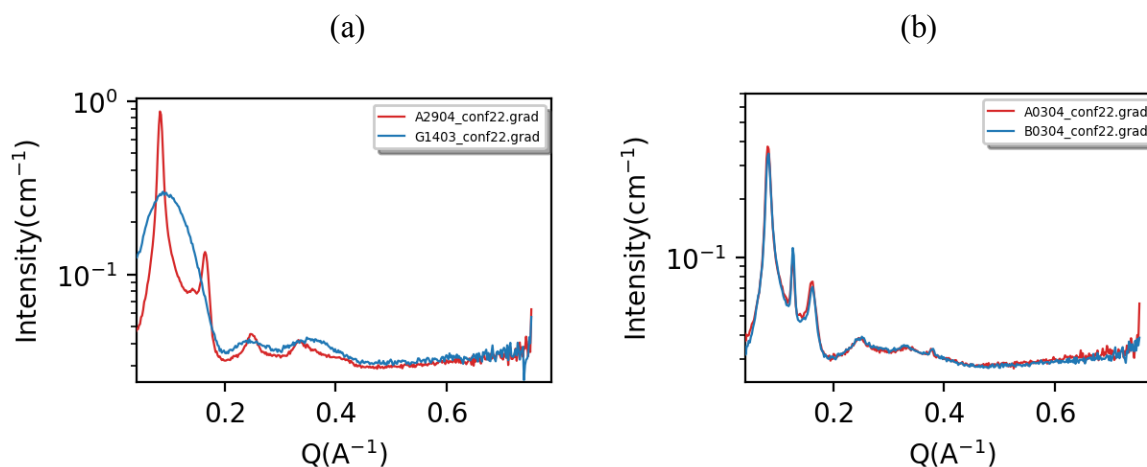


Fig. 9. SAXS curves showing (a) formulation A2904 (without SSL) and G1403 (with SSL) and (b) A0304 (with photosteroyl canola glycerides) and B0304 (without photosteroyl canola glycerides)

4.8 Lead formulation

Table 3 below shows the final lead formulation's ingredients and concentrations; the preparation method is described in Appendix E below. The pH of the final product was 5.5 and

is suitable for skin formulations [3, 21]. Visually the formulation was creamy white and slightly viscous with a good sensory and texture on the skin. Soy HPC1 was chosen as the emulsifier of choice. Pure hydrogenated PCs are more potent emulsifiers compared to those with unsaturated chains and lecithin [9]. This was observed as soy HPC1 and soy HPC2 were relatively easy to handle and easily formed homogeneous emulsions as compared to soy UL and SF UL. Unsaturated soybean PCs are more hygroscopic compared to their saturated counterparts [13]. Soy UL and SF UL absorbed moisture and had poor flow properties making them difficult to handle. More so, unsaturated natural phospholipids are prone to oxidation and addition of antioxidants is necessary during formulation [13], given this, addition of anti-oxidants makes the formulation less clean and increases the cost and risk of changing the microstructure. As a result, these emulsifiers are not good choices for our system as compared to the saturated ones.

The texture and viscosity of formulations made using these hydrogenated PCs were also better compared to the formulations prepared using the non-hydrogenated lecithin. Results from microscopy (Appendix H) shows that the formulation is predominantly made of L_{α} dispersed in an isotropic gel. As reported by Torensca, addition of oil phase disturbs lamellar networks in the system [7] and this was observed in our final formulation where a L_{α} phase in mixture with cubic and gel phases was observed. In the work by Kim et al, L_{α} phases were observed at hydrogenated lecithin concentrations of 0.3 – 3% w/w, this was also the case in this work where L_{α} were observed at 2% w/w soy HPC1 concentration [12].

Table 3. Lead formulation (C2203) ingredients and w/w% compositions used.

Phase	Name / Abbr	Supplier	INCI-name	vikts-% (5g sample)	Mix (g)	Act. Wt (g)	Function
A	Water	Lund University	Aqua	80	4.00	4.01	Water phase
A	SSL	AAK Personal Care	Sodium stearoyl lactylate	0	0		Polar anionic emulsifier
B	BPO	AAK Personal Care	Shea butter triglycerides	15	0.75	0.75	Oil phase
B	BPE	AAK Personal Care	Shea butter ethyl esters	0	0		Texturizer
B	Soy HPC1	AAK Personal Care	Hydrogenated PC	2	0.10	0.1	Emulsifier / texturizer
B	Lanette O	BASF	Cetearyl alcohol	2	0.10	0.1	Stabilizer
B	BPE	AAK Personal Care	Shea Butter triterpene esters	1	0.05	0.05	Bioactive emollient
			pH 5.5				

Fig. 10 below shows the SAXS results of the lead formulation at configuration 21, 22, 23 and the q values and their respective d spacing figures. Hydration of PLs leads to formation of self-assembled liquid crystalline structures, ranging from lamellar, hexagonal to cubic (7). In this work, SAXS and microscopic results showed that these phases are formed at various emulsifier

concentrations in binary and ternary systems. This was also observed in the final lead formulation as shown in SAXS images in Fig. 10 below. The results of SAXS (configuration / detector distance 22 and 23) and WAXS (configuration / detector distance 21) showed the presence of L_α phase in the formulation. The $q_1:q_2:q_3$ ratio of Bragg peaks (1,2,3) was 1:2:3. The peak positions did not change in all configurations and the d spacing based on q_1 was 69\AA showing the interlayer spacing in the liquid crystals. A sharp peak observed at position 2 in the graph could be an indication of gel phase, system like these are usually multiphasic and phospholipids and triglycerides can form gel phases in an emulsion [17]. The reasoning behind this is partially because the peak is very sharp and well defined, which indicates that the structure is very well ordered (more than liquid crystals), typical of gel phases. This is also partially because the phospholipids used in this work have fully saturated tails, which have a high chain melting temperature therefore it is plausible that the tails are not fully melted and are existing in some kind of gel phase. This peak (2) has a q value of 0.183 and d spacing of 34.33\AA as shown in the table in Fig 10 below. This, along with the sharpness of the peak, could also indicate crystalline domains with repeat distance of approximately 34.33\AA .

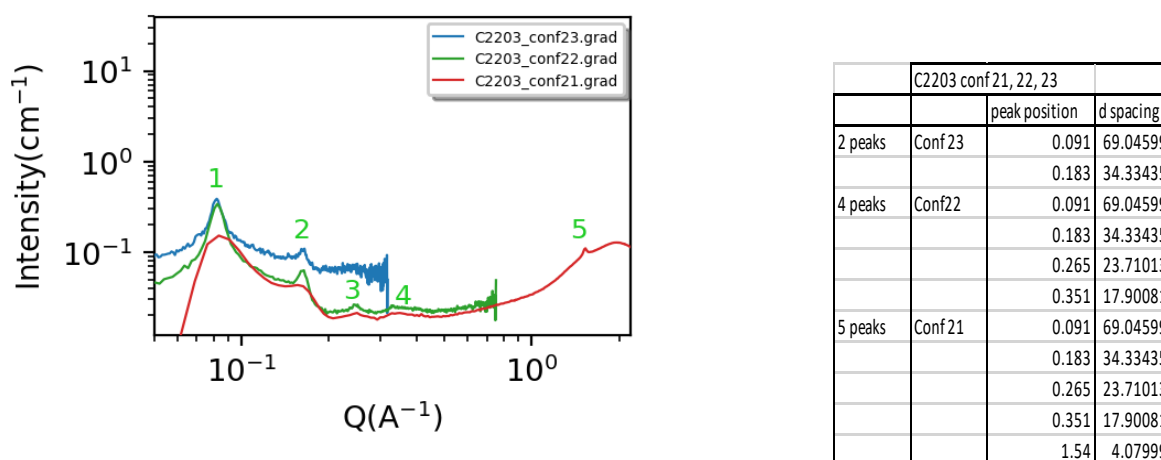


Fig 10. shows (left) X-ray scattering curves at small angle (conf. 22 and 23) and wide angle (conf 21) for lead formulation and (right) peak positions and d spacing calculated values.

The x-ray results at wide angle (conf. 21) showed an additional peak (5) at $q = 0.54$ and the calculated d value was 4.08\AA as shown in Fig. 10 above. This sharp peak indicates presence of ordered crystalline chains and the repeat distance between the chains is 4.08\AA . This peak was also observed on the WAXS results at a temperature of 35°C , which suggests that the chain melting is higher than the body or skin temperature. The lead formulation investigation at 35°C (skin temperature) showed identical SAXS curves (Appendix F), meaning that the

nanostructure of the formulation did not change at skin temperature and therefore the formulation is expected to have structural stability on the skin. At physiological temperature the L_{α} phase is stable for hydrogenated natural phospholipids and the phase transition temperature, when fully hydrated is above 50°C. [13]

The average droplets sizes for the lead formulation were evaluated using light scattering and microscopy, the results can be seen in Fig. 8 and Table 2 above. The average droplets size was 68 μm (SLS) and the particle size distribution was wide as shown by graph in Appendix I. This shows that the polydispersity of the system was very high and this has a negative effect on the stability of the system. However, such a system has better delivery of lipophilic drugs and leads to high bioavailability of active ingredient [8]. Swollen liquid crystalline systems do have a prolonged and sustained release of both hydrophilic and lipophilic drugs [6], this helps improve the efficacy of the formulation.

The interfacial packing of natural PCs is very complex and poses a challenge of predicting the ability of formulations to form stable interfaces and emulsions, it is therefore important to conduct emulsion stability screening experiments. Although the phases of the lead formulations separated after a week, the emulsions could be easily formed by simple shaking. Given the importance of liquid lamellar structures in our system, this emulsion was considered the best. Further development of the emulsions should be done to improve the emulsion stability. Addition of shea ethyl esters and/or SSL was proven to slightly improve the texture and stability; however, the improvement was not very significant and it impacted L_{α} phases and hence a decision was taken to exclude them. It is however worth trying increasing the amount of CA or adding thickeners like carbomer to the system. These additions might however affect the nanostructure, making the formulation less clean and increasing the cost of the formulation. Therefore, careful considerations should be taken when modifying this formulation. Adding more of these ingredients also increases the cost of the formulation. Although more work needs to be done to optimize the formulation, this lead formulation can provide a starting point and direction for development of a highly functional product form commercial purposes.

5 Conclusions

Comparatively, soy HPC1 showed better ability to form liquid lamellar phases and was chosen as more ideal for the formulation. Addition of other ingredients led to a lead formulation that also possessed excellent microstructures that seem adequate to for delivery of bioactive emollients with high functionality (bioavailability) which can lead to better efficacy. The addition of cetearyl alcohol did not alter the microstructure but appeared to help increase the viscosity and stabilize the emulsion. Although SSL had a significant impact on the viscosity and stability of the system, a decision was taken to not include it because it had a significant impact on the microstructure of the emulsion. Loss of L_{α} structure and very high viscosity affects the emulsion's ability to deliver the active ingredients. The addition of shea ethyl esters caused a slight improvement in the sensorial texture of the emulsion. However, a decision was taken to exclude it in the lead formulation to allow exploration of other alternatives like carbomer that improve texture and stability at the same time. Addition of both shea ethyl esters and carbomer in the emulsion leads to unnecessarily high cost of the emulsion.

Therefore, the lead formulation developed was clean and contained a limited amount of ingredients. Microscopic analysis showed liquid lamellar phases and this was confirmed using SAXS. The droplets sizes measured using SLS were relatively large and polydisperse. This agreed with the visual and sensorial observation which showed a milky slightly viscous formulation with a silky cushion feel on the skin. A lead formulation was therefore developed and characterised and the results of this work can help guide future product development with an enhanced performance.

In this work, the ingredients used are mainly derived from natural sources, most people nowadays prefer cosmetic products from natural sources that are produces in a sustainable way. The results of this work can help support United Nations Sustainable Development Goals (UN SDGs) 1, 4, 8, 9 and 10, most consumers of cosmetic products prefer products with good sustainable credentials. The shea kernels used to make oils used in this work are sourced directly from hundreds of thousands of women shea collectors engaged in the sustainability award-winning AAK Kolo Nafaso program set-up in Burkina Faso, Ghana and Ivory Coast. This helps alleviate poverty and improve gender equality. The results of this work fulfil the objectives and the developed formulation has room for further improvement to make it more suitable for the intended purposes.

6 Future aspects

Given the low viscosity and poor stability of the lead formulation, future work should focus on improving these areas. This can be done by increasing the amount of PC in the formulation, increasing amount of cetearyl alcohol in the system, add SSL and/or shea ethyl esters at different amounts than the one already investigated as well as considering addition of thickeners like carbomers. Secondly, it is important to put a sensorial panel to get expert opinions on the texture and sensorial feeling of the skin as well as perceptions on formulations whose phases separate and require shaking before use. Thirdly, further characterization of the formulation using rheology measurements and differential scanning calorimetry is important to further characterise and understand the formulation. It is also unclear why soy HPC2 forms emulsions that are more stable than the purer soy HPC1, this requires further probing. Furthermore, the long-term stability and structural changes need to be investigated. Lastly, the actual release profile and bioavailability of the active ingredients need to be investigated on biological samples like pig skin or other biological models mimicking the human skin.

7 References

1. Ahmad, A. and Ahsan, H., 2020. Lipid-based formulations in cosmeceuticals and biopharmaceuticals. *Biomedical Dermatology*, 4(1). <https://doi.org/10.1186/s41702-020-00062-9>
2. Tolnay, A., Koris, A. and Magda, R., 2018. Sustainable Development of Cosmetic Products in the Frame of the Laboratory Market. *Visegrad Journal on Bioeconomy and Sustainable Development*, 7(2), pp.62-66. DOI: 10.2478/vjbsd-2018-0012
3. AAK Personal Care, Redefine natural, Version 5, 2021. AAK Academy. <http://www.aak.com>
4. Ali, A., Skedung, L., Burleigh, S., Lavant, E., Ringstad, L., Anderson, C., Wahlgren, M. and Engblom, J., 2022. Relationship between sensorial and physical characteristics of topical creams: A comparative study on effects of excipients. *International Journal of Pharmaceutics*, 613, p.121370. <https://doi.org/10.1016/j.ijpharm.2021.121370>
5. Andersson, A., Protection against stress by natural triterpene esters, 2021, AAK Academy. <http://www.aak.com>
6. Montalvo, G., Pons, R., Zhang, G., Díaz, M. and Valiente, M., 2013. Structure and Phase Equilibria of the Soybean Lecithin/PEG 40 Monostearate/Water System. *Langmuir*, 29(47), pp.14369-14379. <http://dx.doi.org/10.1016/j.jcis.2013.07.016>
7. Terescenco, D., Picard, C., Clemenceau, F., Grisel, M. and Savary, G., 2018. Influence of the emollient structure on the properties of cosmetic emulsion containing lamellar liquid crystals. *Colloids and Surfaces A: Physicochemical and Engineering Aspects*, 536, pp.10-19. <http://dx.doi.org/10.1016/j.colsurfa.2017.08.017>
8. Gosenca, M., Bešter-Rogač, M. and Gašperlin, M., 2013. Lecithin based lamellar liquid crystals as a physiologically acceptable dermal delivery system for ascorbyl palmitate. *European Journal of Pharmaceutical Sciences*, 50(1), pp.114-122. <http://dx.doi.org/10.1016/j.ejps.2013.04.029>
9. Nii, T. and Ishii, F., 2004. Properties of various phosphatidylcholines as emulsifiers or dispersing agents in microparticle preparations for drug carriers. *Colloids and Surfaces B: Biointerfaces*, 39(1-2), pp.57-63. doi:10.1016/j.colsurfb.2004.08.017
10. F. Otto, P. Van Hoogevest, F. Syrowatka, V. Heinli, R. H.H. Neubert, 2020. Assessment of the applicability of HLB values for natural phospholipid emulsifiers for preparation of stable emulsions, *Pharmazie*. doi: 10.1691/ph.2020.9174
11. Boggs, J., 1987. *Biochem. Biophys. Acta* 906 353–404.

12. Kim, I., Nakagawa, S., Ri, K., Hashimoto, S., Masaki, H., 2009. Liquid. Crystal o/e emulsions to mimic lipids and strengthen skin barrier function. *Cosmetics and Toiletries* 124(6). www.CosmeticsandToiletries.com
13. van Hoogevest, P., 2017. Review – An update on the use of oral phospholipid excipients. *European Journal of Pharmaceutical Sciences*, 108, pp.1-12. <http://dx.doi.org/10.1016/j.ejps.2017.07.008>
14. Kurukji, D., Pichot, R., Spyropoulos, F. and Norton, I., 2013. Interfacial behaviour of sodium stearyl lactylate (SSL) as an oil-in-water pickering emulsion stabiliser. *Journal of Colloid and Interface Science*, 409, pp.88-97. <http://dx.doi.org/10.1016/j.jcis.2013.07.016>
15. Vengsarkar, P., Roberts, C., 2014. Solid-stabilized emulsion formation using stearyl lactylate coated iron oxide nanoparticles, *J Nanopart Res* 16:2627. doi10.1007/s11051-014-2627-4
16. Du, G., Del Giudice, A., Alfredsson, V., Carnerup, A., Pavel, N., Loh, W., Masci, G., Nyström, B., Galantini, L. and Schillén, K., 2020. Effect of temperature on the association behavior in aqueous mixtures of an oppositely charged amphiphilic block copolymer and bile salt. *Polymer*, 206, p.122871. doi 10.1016/j.polymer.2020.122871
17. Hiemenz, P., 1986. *Principles of colloid and surface chemistry*, 2nd ed., doi10.1177/004051758205200822
18. O Glatter, 2018. *Scattering methods and their applications in colloid and interface science*, Elsevier Inc.
19. Malvern Panalytical, *Dynamic light scattering - common terms defined*, 2022 <https://www.malvernpanalytical.com/en/learn/knowledge-center/whitepapers/wp111214dlstermsdefined>
20. 2004 van Smeden, J., Janssens, M., Gooris, G. and Bouwstra, J., 2014. The important role of stratum corneum lipids for the cutaneous barrier function. *Biochimica et Biophysica Acta (BBA) - Molecular and Cell Biology of Lipids*, 1841(3), pp.295-313. <http://dx.doi.org/10.1016/j.bbalip.2013.11.006>
21. Björklund, S., Andersson, J., Pham, Q., Nowacka, A., Topgaard, D. and Sparr, E., 2014. Stratum corneum molecular mobility in the presence of natural moisturizers. *Soft Matter*, 10(25), pp.4535-4546. doi 10.1039/c4sm00137k
22. Pham, Q., Björklund, S., Engblom, J., Topgaard, D. and Sparr, E., 2016. Chemical penetration enhancers in stratum corneum — Relation between molecular effects and

- barrier function. *Journal of Controlled Release*, 232, pp.175-187.
doi10.1016/j.jconrel.2016.04.030
23. Cosmetics Europe, The Personal Care Association, 2021, Belgium,
<https://cosmeticseurope.eu/cosmetics-industry/>
24. Coupland, J. and Julian McClements, D., 2001. Droplet size determination in food emulsions: comparison of ultrasonic and light scattering methods. *Journal of Food Engineering*, 50(2), pp.117-120.
25. Gore, E., Picard, C. and Savary, G., 2020. Complementary approaches to understand the spreading behaviour on skin of O/W emulsions containing different emollients. *Colloids and Surfaces B: Biointerfaces*, 193, p.111132.
<https://doi.org/10.1016/j.colsurfb.2020.111132>
26. Tardieu, A., Luzzati, V. and Reman, F., 1973. Structure and polymorphism of the hydrocarbon chains of lipids: A study of lecithin-water phases. *Journal of Molecular Biology*, 75(4), pp.711-733. doi 10.1016/0022-2836(73)90303-3
27. Amberg, N. and Fogarassy, C., 2019. Green Consumer Behaviour in the Cosmetics Market. *Resources*, 8(3), p.137. doi:10.3390/resources8030137
28. Du, G., 2022. Versatile Association Behaviour in Mixtures of oppositely charges Amphiphiles. From DNA-Like Assembly of Supramolecular Helices to Coacervation in Chiral Surfactant Systems. <https://portal.research.lu.se/en/publications/d67412ee-c0f0-4e94-bd36-f5b25ce26846>
29. US Pharmacopeia, 2016. Lecithin Official Monographs, USP 39/ NF 34, First Supp.

8 Appendix

Appendix A. Table showing list of all ingredients used in this work.

Name / Abbreviation	INCI Name	Supplier	Batch no.	Function
PCG	Photosteryl Canola Glycerides	AAK Personal Care	2208284	Bioactive emollient
BPE	Butyrospernum Parkii (shea) Butter triterpene ester	AAK Personal Care	2142269	Bioactive emollient
Lanette O	Cetearyl alcohol	BASF, Germany	16411161	Stabilizer
SSL	Sodium steroyl Lactylate	AAK Personal Care	4014054572	Polar anionic emulsifier
BPO	Butyrospernum Parkii (shea) Butter / oil	AAK Personal Care	2142105	Oil Phase
BPB	Butyrospernum Parkii (shea) Butter ethyl ester	AAK Personal Care	2271791	Oil Phase / texturizer
Soy HPC2	Soy hydrogenated phosphatidylcholine (medium purity)	AAK Personal Care		Emulsifier / texturizer
Soy HPC1	Soy hydrogenated phosphatidylcholine (High purity)	AAK Personal Care		Emulsifier / texturizer
Soy UL	Non-hydrogenated lecithin	AAK Personal Care		Emulsifier / texturizer
SF UL	Sun flower lecithin	AAK Personal Care		Emulsifier / texturizer
Water	Aqua	Lund University		Water Phase

Appendix B. Table showing formulations prepared and evaluated during development stages.

FORMULATIONS EVALUATED																							
	C2203	E2203	F2203	B2203	A0304	B0304	C0304	D0304	F0304	G1403	B1404	A1404	B2303	A0704	A2904	B2909	C2909	A2004	B2004	C2004	D2004	E2004	
Soy HPC2				2	2				2				2										
Soy HPC1	2	2				2	2			5	5				2	5	5	5	2	5	10	15	20
Soy UL												2		2									
SF UL								2															
Lanette O	2	2		2		2	2	2	2	2	2	2	2	1	2	2	2	2					
SSL		0.5			0.5						0.5								15	15	15	15	15
BPO	15	15		15	15	15	15	15	15	15	15	15	15	15	15	15	15	15					
BPB											5	5	5			5							
BPE	1	1																					
PCG				1	1	1		1	1	1		1	1	1	1	1	1						
Water	80	79.5		80	79.5	80	81	80	80	77	72.5	75	75	80	75	77	77	77	83	80	75	70	65

Appendix C. Table showing the compositions for binary phase screening of lecithins.

BINARY SYSTEM SAMPLES																					
	1A	1B	1C	1E	C1404	4A	4B	4C	4D	4E	E1404	D0704	A2804	B2804	C2804	D2804	E2804	G1404	F1404	C1404	
Soy HPC2	2	20		40	10	5															
Soy HPC1														2	5	10	20	40	5	2	20
Soy UL							2	20	40	50	10	5	10								
Water	98	80		60	90	95	98	80	60	50	90	95	90	98	95	90	80	60	95	98	80

Appendix D. Tables phases formed in the binary phase screening, top (soy HPC2), bottom (Soy UL)

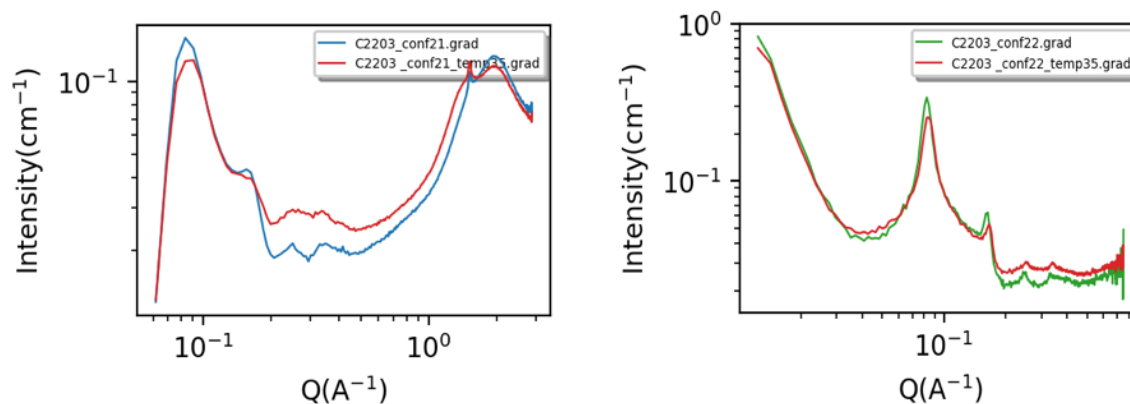
	Micellar Cubic (C)	Lamellar (L)	Lamella gel (G)	Mixed C + L	Mixed L + G
Soy HPC2 % in water					
2				✓	
5		✓			
10		✓			
20					✓
40					✓

	Micellar Cubic (C)	Lamellar (L)	Lamella gel (G)	Mixed C + L	Mixed L + G
LC % in water					
2	✓				
5	✓				
10		✓			
20		✓			
40					✓

Appendix E. Table showing the lead formulation compositions and preparation method.

Name of formulation: C2203				Sample size: 5g			
Phase	Name / Abbr	Supplier	INCI-name	vikts-% (5g sample)	Mix (g)	Act. Wt (g)	Function
A	Water	Lund University	Aqua	80	4.00	4.01	Water phase
A	SSL	AAK Personal Care	Sodium stearyl lactylate	0	0		Polar anionic emulsifier
B	BPO	AAK Personal Care	Shea butter triglycerides	15	0.75	0.75	Oil phase
B	BPE	AAK Personal Care	Shea butter ethyl esters	0	0		Texturizer
B	Soy HPC1	AAK Personal Care	Hydrogenated PC	2	0.10	0.1	Emulsifier / texturizer
B	Lanette O	BASF	Cetearyl alcohol	2	0.10	0.1	Stabilizer
B	BPE	AAK Personal Care	Shea Butter triterpene esters	1	0.05	0.05	Bioactive emollient
			pH 5.5				
1	Mix and prepare phases A and B separately						
2	Heat water and oil phase separately to 80°C						
3	Pour oil phase to water phase						
4	Mix at medium speed (ultra turrax, 6500rpm) for 5 mins						
5	Homogenize						
6	Cool to 25°C while stirring						
7	Check pH						
8	Finish						

Appendix F. SAXS images for lead formulation (C2203) at 25 °C (ambient temperature) and 35 °C (skin temperature)

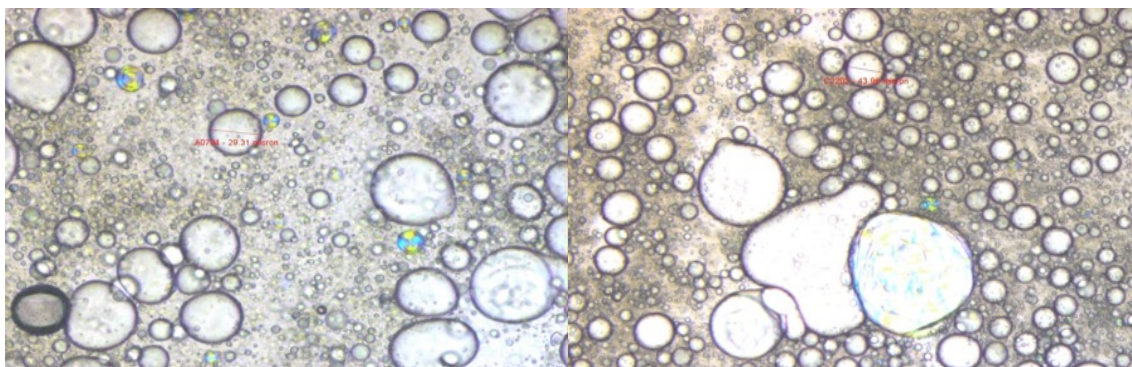


Appendix G. Tables showing binary (left) and ternary (right) phases calculations of *d* spacing for soy HPC2.

	q	d
Peak 1	0.09	69.81317
Peak 2	0.186	33.78057
Peak 3	0.277	22.68298
Peak 4	0.368	17.07387
Peak 5	0.457	13.74876

	q	d
Peak 1	0.09	69.81317
Peak 2	0.141	44.5616
Peak 3	0.186	33.78057
Peak 4	0.277	22.68298
Peak 5	0.368	17.07387

Appendix H. Microscopic images for sample prepared using soy HPC1, the sample on the left (droplet size 29.91nm) contains shea ethyl esters and the sample on the right (droplet size 43.98nm) does don't contain ethyl esters



Appendix I. Graph showing the droplets size distribution for lead sample C2203.

